ELSEVIER

Journal of Materials Processing Technology 178 (2006) 369–378

Journal of Materials Processing Technology

www.elsevier.com/locate/jmatprotec

Optimising the gas-injection moulding of an automobile plastic cover using an experimental design procedure

Miguel Sánchez-Soto [a,*], Antonio Gordillo [a], B. Arasanz [a], J. Aurrekoetxea [b], L. Aretxabaleta [b]

[a] *Centre Català del Plàstic, Universitat Politècnica de Catalunya, c/Colom 114, 08222 Terrassa, Spain*
[b] *Mondragon Goi Eskola Politeknikoa, Mondragón Unibersitatea, 20500 Mondragon, Spain*

Received 3 June 2005; accepted 19 April 2006

Abstract

The main objective of this work was to optimise the production of a plastic automobile door plastic cover using computer simulation and the application of statistical experimental design. Due to the thickness and cover dimensions, the full-shot gas-assisted injection moulding was considered the most suitable manufacturing process. Different fabrication possibilities were investigated changing either the melt or the gas-injection point location. The best alternative was achieved with a sole central point injecting the melt and two adjacent lateral points applying gas. Two overflow channels were situated in part edges to collect the melt displaced by the gas. The experimental design technique was carried out to obtain the combination of variables that provide a greater channel voiding and better thickness uniformity. Gas channels were found to be completely empty after carrying out the simulation, implying that part fabrication was assured, although differences in wall thickness along the channel path were however detected. Results showed that no control of wall thickness was possible through the selected processing parameters. Regarding the displaced melt volume and part weight the controlling parameters were the melt temperature, mould temperature and gas pressure.
© 2006 Elsevier B.V. All rights reserved.

Keywords: Gas-injection moulding; Experimental design; Modelling; Simulation

1. Introduction

The injection moulding is a high-speed automated process widely used to manufacture plastic parts of very different shapes. The parts produced by this process range from small to very large components. This flexibility and the possibility of producing very complicated components have contributed to making injection moulding one of the most important plastic processing methods.

The production of thick-walled plastic components by conventional injection moulding generally presents a great number of problems such as sink-marks or internal voids, thus involving a long processing time [1,2]. To avoid such difficulties, techniques such as gas-assisted injection moulding (GAIM) have been developed. Some of the gas-injection process advantages are a reduction in weight and cycle time, the absence of sink-marks and a low part warp. However, one of the main remaining problems is the control of the plastic voiding and wall thickness especially when dealing with very long components.

Two possibilities for gas-assisted injection moulding are normally used, the short-shot and the full-shot processes. In the short-shot filling process a gas is introduced into a mould that has been partially filled with polymer melt (about 70–90 vol.%) with the aim of first of all, removing the part core and then reduce the part volumetric contraction that occurs during the cooling phase. In the full-shot filling process the gas is introduced once the melt has reached the 100 vol.% of the complete filling. Gas flows following the lower resistance path inward towards the central and still unfrozen section of the previously injected polymer and exerts pressure outwards, packing the polymer melt layer against the mould wall. Gas penetration during the gas-assisted filling stage is known as primary gas penetration. During the post-filling stage the gas can continue penetrating as a result of melt shrinkage; this penetration is termed secondary penetration. When the polymer hardens the gas is removed through the machine or mould nozzle and pressure is released. Finally, the product is cooled down until its temperature is low enough to be ejected without distortion. The results are components with hollow inner channels.

* Corresponding author. Tel.: +34 937 837 022; fax: +34 937 841 827.
E-mail addresses: m.sanchez-soto@upc.edu, m.sanchez-soto@upc.es (M. Sánchez-Soto).

0924-0136/$ – see front matter © 2006 Elsevier B.V. All rights reserved.
doi:10.1016/j.jmatprotec.2006.04.122

The instant of gas inlet is normally delayed from the melt injection and could take place either together with the polymer, at the same injection point, or separately from the melt injection point. Melt and gas-injection points are strongly related as they determine the course of the gas bubble. In this sense, Avery [1] and Ehritt and Schröeder [3] pointed out that the gas nozzle design and location are critical to achieve an optimum gas-injection process. To avoid the gas blowing off through the part skin, the polymer must cover the gas nozzle prior to its introduction and the applied gas pressure should be maintained within a lower range.

Although many experimental researches have been carried out to elucidate the influence of the different variables on the GAIM process [4–7], the relative importance of each variable has not been clearly established. Recently, Li et al. [5] studied the gas penetration in short-shot GAIM as a function of several process parameters, comparing the simulation of a proposed model with the simulation obtained by C-MOLD [9]. Regarding gas penetration, results showed that greater values were achieved when the melt temperature and the delay time between melt and gas introduction were raised. On the other hand, lower values of short size and melt injection speed contributed to an increase in the gas path. Finally, the gas pressure was found to be of minor importance. Liu and Chang [6] pointed out that in full-shot GAIM greater gas penetration was obtained when melt temperature, gas-injection delay time and gas holding time were increased. Studying the secondary penetration in ribs Yang et al. [7] showed that the most critical parameters were the melt temperature and the gas delay time. Gas penetration length was found to increase with melt temperature, mould temperature and gas pressure. The effect of the gas delay time was the opposite.

The fabrication of the cover is planned to be carried out by a full-shot GAIM process but using overflow channels. These channels are placed and designed with the aim of collecting the melt pushed forward by the gas. A valve which opens at the moment of gas inlet switches the entrance to the channels. This procedure is mostly a short-shot GAIM but in some aspects can be considered a combination of the short-shot and full-shot GAIM, so for this reason the set of variables with an influence on the process can be related either to melt or gas injection. The aim of this study was to improve the quality of the automobile cover preventing the principal manufacturing defects that could appear and also to find an appropriate combination of variables to help part injection. Because of this, we decided first of all to optimise the melt-injection process and then to study the action of the gas. The set of variables under consideration was the gas pressure, melt temperature, mould temperature, gas delay time and the time of gas application. The effect of each variable was considered throughout the design of the experiments.

The design of the experiments (DOE) is a powerful tool for determining how a system responds to controlled changes in some inputs or factors, by the observation of the corresponding changes in the responses or outputs. It is considered an appropriated research tool to deal with problems with many interacting variables and it is successfully used to identify and quantify the principal system variables and their effects. The methodology and characteristics of DOE are well established and a large amount of general and detailed information is available throughout [10,11]. Several types of experimental designs can be carried out. A simple design is the variation of only one factor level (or variable) at a time while keeping the remaining of factors constant. The full factorial design uses all possible combinations of levels and factors, therefore all possible variable interactions are included, it is, however, too costly in terms of experiments, time and resources. The fractional factorial design is used to reduce the number of experiments of the full factorial design. This procedure allows the optimisation of the number of experiments to be completed, although some interactions may be lost and additional runs may be necessary.

In this work, the global gas-assisted injection moulding simulation was split as follows. The process started with the optimisation of the complete polymer injection, simulating several alternatives for the melt inlet location. The best location was then chosen following the rule of minimum impact on part quality and in terms of manufacturing straightforwardness. Aspects like melt flow advance, the presence or absence of weld lines, the temperature distribution and also the complexity of mould execution were considered. Once the melt point entrance was defined, three different gas-injection points were evaluated. Each one of the gas alternatives was coupled with the previously defined melt injection point and then global simulation was carried out. Finally, the effects of the most important process variables on the GAIM process were studied by a fractional design of experiments. The response was focussed on the part weight, the volume of melt removed, and the control of the remaining plastic wall thickness along the gas channel.

2. Component definition and environment

The position and situation of the studied component inside the car is shown in Fig. 1. The component is located at the top of the rear automobile door and its primary function is decorative by covering the metallic structure profile. In addition, to improve the appearance of the interior car space, the plastic cover must allow electric wires to be hidden inside. The principal component difficulty lies in its complex geometry. Due to its long u-shaped profile it has a very low rigidity. Furthermore, the assembling process is manual and requires the part to bend along its central axis, so excessive rigidity is undesirable to prevent early fractures. As shown in Fig. 2 the component is considerably long causing the melt to flow along a long path to complete the filling. Thus, different melt gating options having different melt paths were simulated in order to assure the total part filling.

Rib reinforcement was not allowed because of part bending. On the other hand, if the part were made by conventional injection moulding, it would be very thick and superficial defects could appear. To solve this problem, a gas-channel was thought out to follow the path indicated by a dotted line in Fig. 2. The section of the foresight gas-channel section is not constant showing the minimum thickness at the centre of both sides and progressively becoming thicker at the part ends. The maximum channel section is located in the part corners. Although the generally recommended design procedure is to place a con-

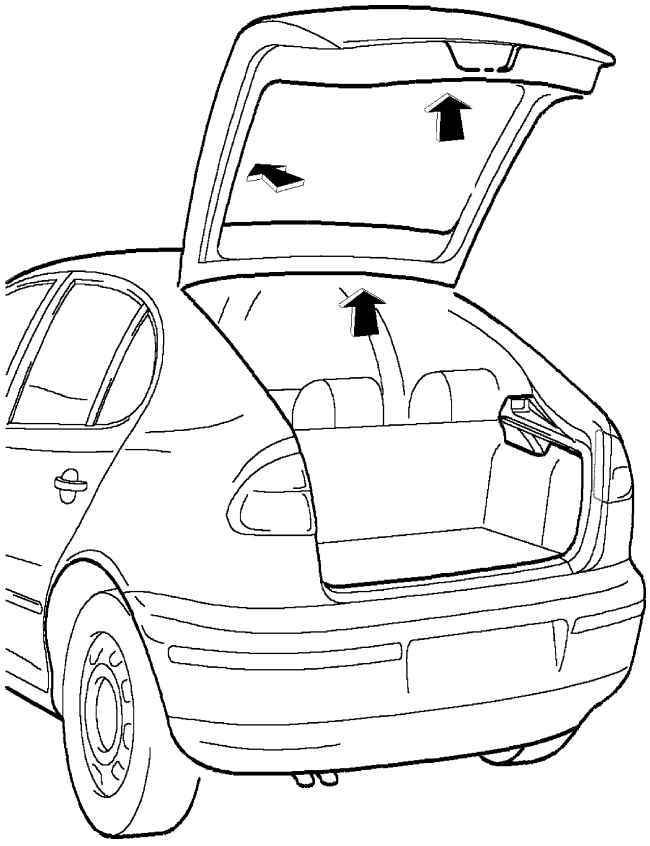

Fig. 1. Situation of the part in the automobile.

stant gas-channel section, this rule cannot be applied here. If a big channel were designed, the net mechanical resistance at the bending zone would become insufficient to support the bending stresses developed during the assembly process causing failure or damage. On the other hand, if a small channel were designed, it would probably result in external defects around the part corners.

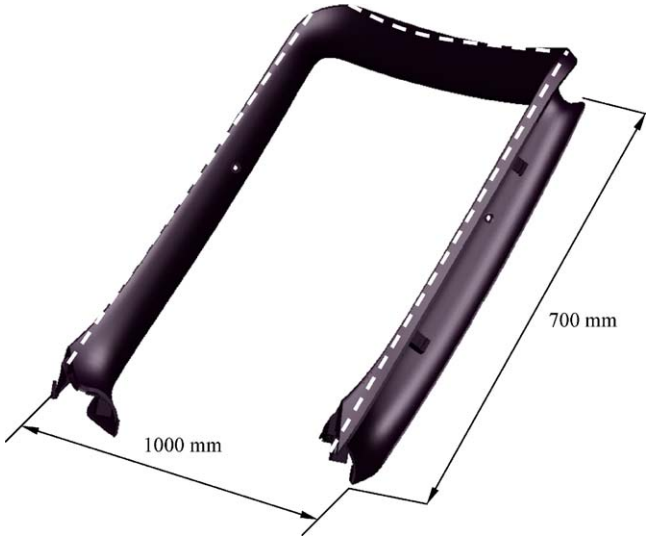

Fig. 2. Part geometry and dimensions. Dotted line represents the desired gas channel path location at the inner side of the part.

3. Material modelling

3.1. Polymer characterisation

A thermoplastic polypropylene copolymer Hostacom X4323/2S68 grade manufactured by Basell (Basell Polyolefins Ibérica S.A., Barcelona, Spain) was selected as suitable material for the injection moulding. This grade is heat and ultraviolet light exposure stabilised and fulfils the standards for flammability [12]. Another important feature of this material is its low odour absorption, which is very important as the designed part is located in the automobile cockpit. The material is reinforced by a 20% in weight of talc.

The simulation process requires the knowledge of material properties like heat capacity, heat conductivity, thermal expansion coefficient, viscosity and pressure–volume–temperature (PVT) curves. The heat capacity, heat conductivity and thermal expansion are functions of the polymer temperature. These sets of curves were extracted from the C-Mold® database [9].

The polypropylene viscosity shows two regimes of flow behaviour, Newtonian and shear-thinning. The Newtonian flow occurs at low shear rates and the shear-thinning behaviour takes place when increasing the shear as the viscosity tends to fall away. To describe the rheological behaviour of melt polypropylene the Cross–William–Landel–Ferry (Cross–WLF) model was applied [13]. This model provides an accurate description of the polymer viscosity over a wide range of shear velocities even for low shear velocities which could be developed during the holding pressure stage. The Cross–WLF model treats polymer viscosity as a function of temperature (T), pressure (p), and shear rate ($\dot{\gamma}$). The model needs seven constants to be introduced (n, τ^*, D_1, D_2, D_3, A_1, A_2), it is described by the following expressions:

$$\eta = \frac{\eta_0}{1 + \left(\frac{\eta_0 \dot{\gamma}}{\tau^*}\right)^{1-n}} \tag{1}$$

where τ^* is the shear stress, $\dot{\gamma}$ the shear rate, n a constant, η the viscosity and η_0 is the viscosity extrapolated to a zero shear stress that can be expressed by

$$\eta_0 = D_1 \exp\left[-\frac{A_1(T - T^*)}{A_2 + (T - T^*)}\right] \tag{2}$$

and

$$T^* = D_2 + D_3 p \tag{3}$$

$$A_1 = A_2 + D_3 p \tag{4}$$

In the preceding equations D_1, D_2, D_3, A_1 and A_2 are constants, p the exerted pressure, T the melt temperature, and T^* is normally taken equal to the glass-transition material temperature. D_3 is introduced to characterise the linear dependence of T^* with pressure. In our case this dependence is considered negligible and thus D_3 is zero. In this case, D_2 then receives the value of the polymer glass transition temperature found at low pressure (0.1 MPa). The values of the constants for the Hostacom

Table 1
Constant values of Cross–WLF model for Hostacom X4323/2S68

n	0.2852
τ^* (Pa)	3.56E+4
D_1 (Pa s)	4.577E+12
D_2 (K)	263.1
A_1	27.17
A_2 (K)	51.6

X4323/2S68 used in the gas-injection simulation are shown in Table 1.

The PVT curve shows the dependence of specific plastic melt volume on pressure and temperature making it possible to follow the polymer shrinkage during the in-mould cooling process. The polypropylene PVT curves were kindly supplied by Targor (Targor plásticos S.A., Barcelona, Spain) and are shown in Fig. 3. Once the PVT curves were obtained, they had to be introduced into the simulating program as a set of equations. We used the two-domain modified Tait equation. The application of this equation to model the PVT curves has been studied by Chiang et al. [14], Hartmann et al. [15,16], and Jain and Simha [17]. Following this, the variation of the specific melt volume is expressed by

$$v = v_0 \left(1 - 0.894 \ln\left(1 + \frac{p}{B}\right)\right) + v_t \tag{5}$$

where p is the acting pressure and, v_0, v_t and B are defined below depending on melt temperature. If the polymer melt temperature is higher than the temperature of crystallisation the following relations apply

$$v_0 = b_{1m} + b_{2m}(T - b_5) \tag{6}$$

$$B = b_{3m} \exp[-b_{4m}(T - b_5)] \tag{7}$$

$$v_t = 0 \tag{8}$$

In other cases, the valid equations are:

$$v_0 = b_{1s} + b_{2s}(T - b_5) \tag{9}$$

$$B = b_{3m} \exp[-b_{4s}(T - b_5)] \tag{10}$$

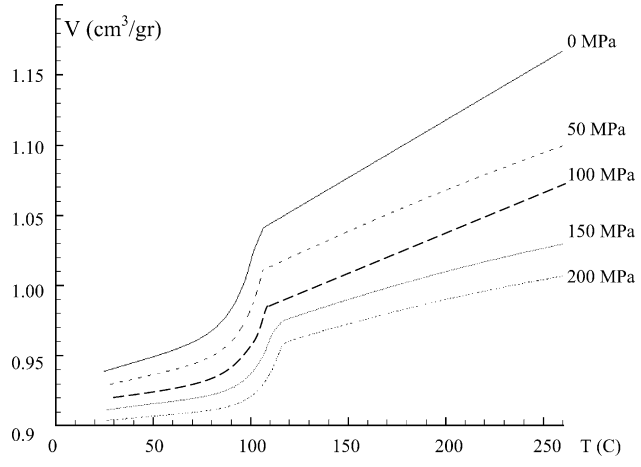

Fig. 3. PVT curves for Hostacom X4323/2S68.

Table 2
Tait constant values for Hostacom X4323/2S68

Factor	
Liquid phase	
b_{1m}	0.00104 $m^3\,kg^{-1}$
b_{2m}	8.20E−7 $m^3\,kg^{-1}\,K^{-1}$
b_{3m}	1.331E+8 Pa
b_{4m}	0.00568 K^{-1}
b_5	377.1 K
b_6	6.801E−8 $K\,Pa^{-1}$
b_7	6.932E−5 $m^3\,kg^{-1}$
b_8	0.0958 K^{-1}
b_9	7.833E−9 Pa^{-1}
Solid phase	
b_{1s}	0.0097 $m^3\,kg^{-1}$
b_{2s}	3.928E−7 $m^3\,kg^{-1}\,K^{-1}$
b_{3s}	2.051E+8 Pa
b_{4s}	0.00783 K^{-1}

$$v_t = b_7 \exp(b_8 T - b_9 p) \tag{11}$$

Finally, the transition temperature is taken from the crystallisation temperature and considering a linear pressure relationship;

$$T = b_5 + b_6 p \tag{12}$$

The constants b_{im} and b_{is} are associated with the expansion thermal coefficients in liquid and solid phases, respectively. The factor b_5 is used to represent the jump in the specific volume found at the crystallisation temperature. The remaining constants, b_7, b_8 and b_9, are adjusting coefficients. The values of the Tait constants for the polypropylene are shown in Table 2.

3.2. Machine, mould and gas definition

The injection-moulding machine was selected taking into account the clamping force necessary to compensate the reactive force developed in the part cavity. The injection machine simulated was a Battenfeld having 1800 t of clamping force. The mould was simulated introducing the thermal characteristics of steel given in Table 3 in the program. For the injected nitrogen gas, the properties were assumed to be constant within the processing conditions considering only the gas pressure as an input factor.

3.3. Gate effects and meshing details

In the development of expressions relating to wall shear stress and pressure drop for a polymer pushed through a capillary hole it is usually assumed that the flow is fully developed along the entire tube length. However, a more accurate approach should

Table 3
Properties of mould steel

Property	Steel
Density ($kg\,m^{-3}$)	7820
C_p ($J\,kg^{-1}\,K^{-1}$)	460
λ ($W\,m^{-1}\,K^{-1}$)	36.5

Table 4
Processing variables or input factors to analyse

Factor	Levels		
	−1	0	1
Melt temperature, T_m (°C)	200	215	230
Mould temperature, T_{mld} (°C)	40	55	70
Gas pressure, P_g (MPa)	8	10	12
Delay time, t_d (s)	2	3	4
Time of gas application, t_g (s)	15	20	25

account for the entrance effects occurring at both ends of the tube. In the GAIM process these losses take place, for example, when the polymer melt enters into the part coming from the gates or when it is pushed away into the overflow tank. To consider this phenomenon the Bagley correction [18] was used. This correction relates the pressure loss (Δp) as a function of the shear stress (τ^*). For polypropylene, its equation takes the following form:

$$\Delta p = 3.6 \times 10^{-5}(\tau^*)^{2.098} \quad (13)$$

The geometry of the part was separated into several elementary surfaces linked at theirs edges. The created surfaces were automatically meshed using 6600 three-node triangular elements. Each element had 14 pile-up layers that were used to model the through-the-thickness flow behaviour ($2D^{1/2}$ simulation). Care was taken during meshing to avoid distorted elements.

4. Experimental procedure

Initially, several simulation runs where carried out to optimise the melt injection. Once the melt injection was defined, global simulation runs including gas action were performed.

Five processing parameters were examined to study the effects of processing conditions on the cover. These parameters or input factors were gas pressure (P_g); melt temperature (T_m), mould temperature (T_{mld}), gas delay time (t_d) and the time of gas application (t_g). The factor levels (Table 4) were selected according to the part and material characteristics and considering the results of the initial simulation. The responses measured in the experiments were chosen in accordance to their importance regarding part hollowing and also taking previous experiences into consideration [19]. Therefore, the amount of channel voiding (V_c), the final part weight (W) and the polymer layer thickness through the channel path at initial (T_1) medium (T_2) and final (T_3) position were studied.

Due to part and mould restrictions, practical GAIM experiences on the injection-moulding machine could not be carried out. Because of this simulation results were compared with the part once it was completely manufactured.

A 2^{5-1} fractional design plus a central value replica was carried out making up a total of 17 experiments. Three and four order interactions were not considered and experiment randomisation was done.

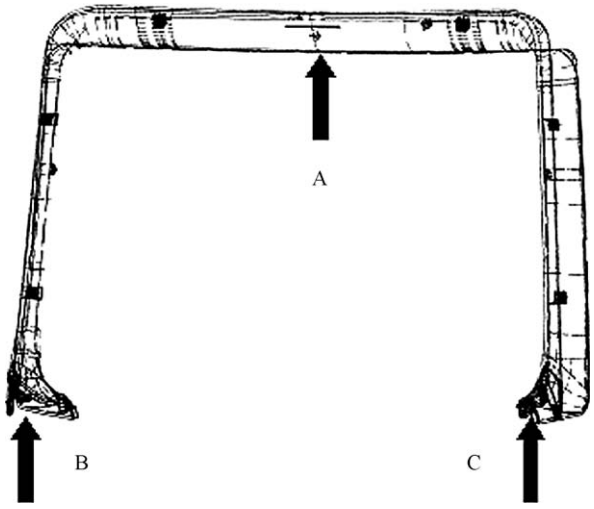

Fig. 4. Melt gating options superimposed over the frontal part view.

5. Results and discussion

5.1. Simulations of polymer melt injection

In the first step of the simulation we considered the three gating options represented in Fig. 4. The option with a unique gate in the centre (gate A) was technically the simplest and mould execution results also easy, but this solution had one of the longest melt flow paths, implying an important pressure drop during the injection moulding. This fact, can be appreciated by the need to apply the highest injection pressure and highest clamping forces of the considered alternatives (Table 5). The temperature gap between two extreme points, one located near the gate and the other located in the coolest part position, was considerably high. The difference was of approximately 90 °C in the case of option A, this being a warning signal of post-moulding deformations. Despite this, the lower temperature region is placed in the middle of one of the cover arms. Therefore, when melt reaches the end of the mould it stops and cools down very quickly but without affecting the filling of the remaining part. Furthermore, it should be taken into account that part of the temperature difference can be attributed to a local melt heating produced by friction and shear at the gate entrance.

In the vicinity of the gate the shear stress ratio reached its maximum of 0.23 MPa, meaning that the simulated conditions in this area were close to that of material degradation the limit of which being about 0.25 MPa. The flow lines obtained after the simulation showed that melt tends to move forward faster through the gas channel than across the part thickness. However, near channel positions no sign of plastic back flow were detected.

Table 5
Comparison of results obtained for the different gating injection alternatives

Gating option	Injection pressure (MPa)	Clamp force (t)	Shear ratio (MPa)	Maximum temperature gap (°C)	Temperature gap at weld line (°C)	Weld lines
A	52.8	433	0.23	90.0	–	0
B + C	41.1	313	0.15	91.4	34	1
A + B + C	26.5	171	0.12	97.4	58	2

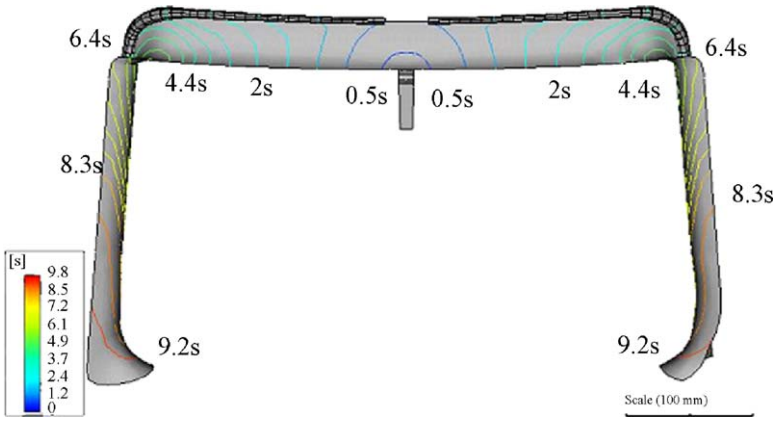

Fig. 5. Melt flow path obtained after simulation for the case of a central melt gate. Numbers indicate the time at which the isochronal flow line reaches that position.

The double gating option (gates B + C) yields less reactive forces in the mould because the flow path is reduced, but the hazard of a weld line arises. As melt enters simultaneously through part edges, the weld line will be situated just at the front cover over the bending region. The triple gating option (gates A + B + C) results in a minimum level of injection pressure and clamping force but a maximum temperature gap and much more complicated mould execution. In this latter configuration, two welding lines appear on both sides of the cover affecting thus to aesthetic.

In both cases the weld lines are formed once the plastic melt has travelled down half of the cover, arriving at the junction area in a relatively cold state with a decrease in temperature of 34 °C in the B + C gating option and 58 °C in the A + B + C gating option. Therefore, apart from an aesthetic danger, the weld line region has a high risk of in-service failure because both fluxes of polymer melt will not properly intersperse. Thus, taking the previously mentioned risk of failure into consideration, the selected solution for melt injection was a unique central gate point. The filling paths for a unique gate (Fig. 5) show a uniform melt front advance. Isochronal lines in the gate vicinity are closer than in both laterals where melt velocity tends to decrease. As said before, the part flow is not fully balanced because flow arrives at the right end corner before the left end corner. However, this difference is small and will not affect the part manufacturing process or the part appearance. The pressure evolution showed similar trends as the melt flow path.

5.2. Gas-injection simulation

Once the melt injection point was defined, the optimum point for gas-inlet had to be selected. In all cases the condition for a successful gas location was to achieve a completely channel hollowing. We finally considered the three possibilities represented in Fig. 6. We used hydraulic controlled overflow vessels to collect the displaced polymer. The vessel valves open the moment they get in contact with the melt flow.

In the first configuration (Fig. 6a) the polymer melt temperature near the injection point was the highest. Polymer melt viscosity decreases with temperature so the proximity between melt and gas-injection points facilitates gas penetration into the polymer. As a result, the gas movement was constant and almost regular through the whole part length. There was a risk of gas intrusion into unwanted part areas. This intrusion, known as finger effect, can produce a rough exterior surface or even holes. The finger effect was effectively detected in the simulations as can be appreciated in Fig. 7a. A local thickness decrease, an increase in the gas channel diameter or a slight separation of the gas inlet points from the melt gate are possible solutions to solving this problem. Under the configuration shown, near the injection gate approximately 65% of the volume was plastic with a 35% voiding.

In the second option (Fig. 6b) the gas inlet points were far away from the melt injection point. In this situation, the polymer melt cooled off making it impossible to achieve a complete hollowed-out part. The simulation shows that the plastic

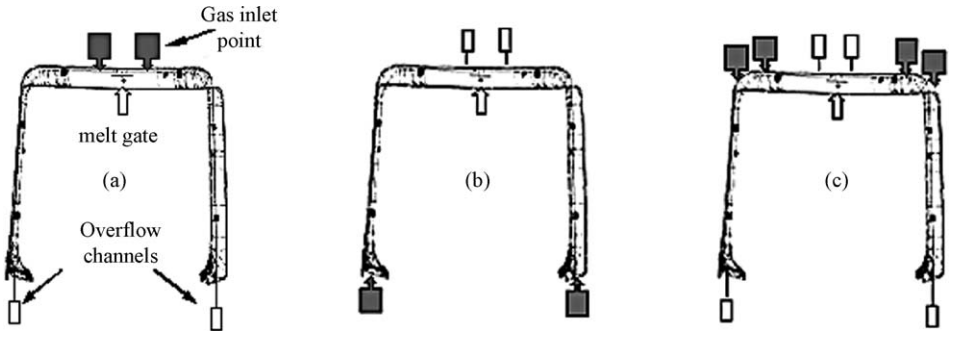

Fig. 6. Gas-injection alternatives.

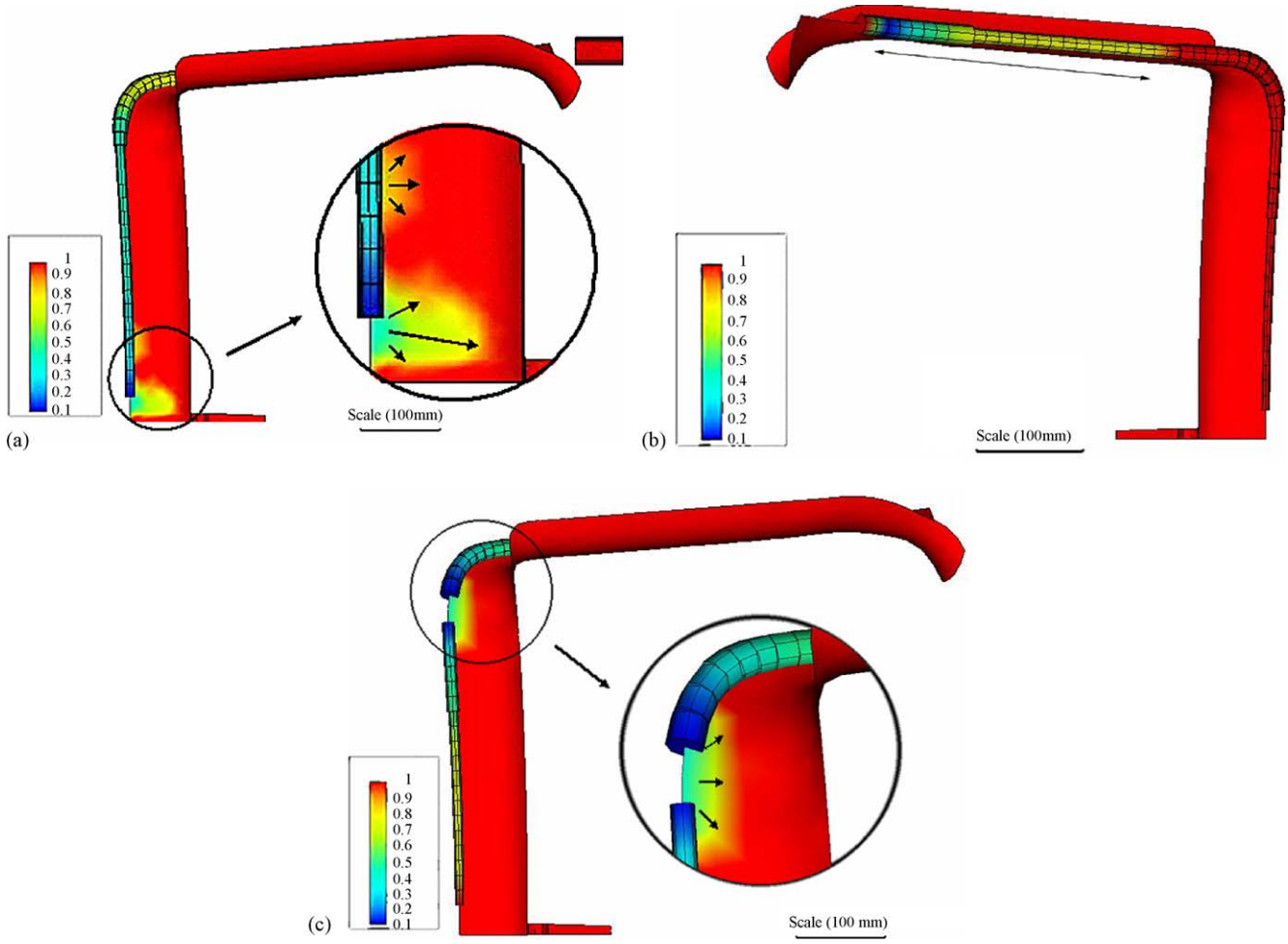

Fig. 7. Gas-injection simulation results. (a) General view of half of the part and detail of finger effect near the melt gate. Arrow indicates the position of gas intrusion. Lateral scale indicates the fraction of volume filled with polymer melt. (b) Detail of partial channel voiding or short-shot. Arrow indicates the length of channel voiding. Lateral scale indicates the fraction of volume filled with polymer melt. (c) Gas jump between two close together gas channels. Inside the circle is detailed the melt path. Lateral scale indicates the fraction of volume filled with polymer melt.

section had been frozen approximately two seconds after the gas-injection (Fig. 7b).

The third alternative (Fig. 6c) had the shorter gas channels, which allows the best part hollowing control. However, the short distance between the channels caused the gas to jump from one channel to the other through the flat plastic sections with a possible gas breakthrough thus implying a change of design to overcome this defect (Fig. 7c). Furthermore, the mould execution was very complex.

As a result, the best part performance was achieved with two gas-injection points located centrally and opposite the injection point, and two overflow channels at the part edges (option 'a' of Fig. 6). In this configuration, the gas was capable of entirely removing the polymer melt, but the skin part thickness was not constant along the entire channel profile, although differences were small.

5.3. Optimisation of the gas-injection process

Once the best melt and gas-injection alternative was established, the simulation was applied to select the set of variables which have an influence on the manufacturing process. The array of experimental results is presented in Table 6.

The Pareto chart represented in Fig. 8 plots the standardised effect on the x-axis and the source of the effect on the y-axis. In terms of the total part weight, it can be appreciated that both melt and mould temperatures have a critical influence, while the rest of the controlled factors have no effect. In the same way, no important interactions between variables seem to have any relevance. In terms of normalised values, the equation relating the part weight with melt temperature and mould temperature has the following expression:

$$W = 951.859 - 4.66T_{\mathrm{m}} - 5.74T_{\mathrm{mld}} \quad (14)$$

The above equation explains the 99.86% of the W variability. To obtain the minimum part weight, the mould and melt temperature should be raised to their highest levels. This fact is reasonable because higher levels of both variables contribute to diminishing the melt viscosity, or to having a reduced melt viscosity inside the mould for a longer time period. Therefore, the transversal void section increases but the gas penetration tends to decrease.

Table 6
Array of experimental results showing input parameters and responses

Run	Input parameters					Responses				
	T_m (°C)	T_{mld} (°C)	P_g (MPa)	t_d (s)	t_g (s)	Part weight, W (g)	Channel voiding, V (%)	Channel thickness, T_1 (mm)	Channel thickness, T_2 (mm)	Channel thickness, T_3 (mm)
1	200	40	8	2	25	962.0	50.08	1.50	5.06	7.08
2	200	40	12	2	15	962.7	64.38	1.41	3.34	6.93
3	230	40	8	2	15	952.9	61.63	0.93	3.34	6.93
4	230	40	12	2	25	952.9	86.43	0.93	3.34	6.93
5	200	40	8	4	15	962.0	51.04	1.50	5.01	7.08
6	200	40	12	4	25	962.2	61.20	1.50	3.34	6.79
7	230	40	8	4	25	952.8	60.03	1.41	3.34	6.93
8	230	40	12	4	15	952.8	80.89	1.41	3.34	6.52
9	200	70	8	2	15	950.7	52.86	0.84	4.91	11.8
10	200	70	12	2	25	950.7	85.78	0.84	3.32	11.8
11	230	70	8	2	25	941.2	78.75	0.84	3.34	7.23
12	230	70	12	2	15	941.2	98.55	0.45	3.29	6.79
13	200	70	8	4	25	950.7	54.89	0.93	3.64	7.23
14	200	70	12	4	15	950.7	81.43	0.93	3.33	7.08
15	230	70	8	4	15	941.7	64.41	0.84	3.37	7.08
16	230	70	12	4	25	941.7	91.49	0.84	3.32	7.23
17	215	55	10	3	20	952.5	71.26	1.32	3.34	6.93

T_m, melt temperature; T_{mld}, mould temperature; P_g, gas pressure; t_d, delay time; t_g, time of gas application. T_1 is the channel thickness measured just at the gas gate. T_2 and T_3 are the channel thicknesses measured at medium and end positions of the gas channel path.

The volume of melt removed by the gas was found to be dependant on three variables; gas pressure and melt and mould temperatures. A lineal interaction between the gas pressure and the mould temperature was also found to be relevant and was included in Eq. (15). In the case of part voiding, gas pressure takes importance because the melt from the part is displaced to the overflow tanks. If the gas pressure is raised, the gas pushes over a greater section of melted polymer, yielding narrow polymer walls and a short penetration length. Lower pressures will render longer gas penetration but narrower hollow sections with the global result of a lower displaced volume of melt. The combinations of higher melt temperatures, mould temperatures and gas pressures will increase both penetration lengths and voiding sections, increasing the total voiding volume. Logically, the final part weight was found to depend on the same variables.

The regression equation which expresses and optimises the relationships between the variables and voiding volume is

$$V = 70.29 + 11.02P_g + 7.54T_m + 5.77T_{mld} + 2.257P_gT_m \quad (15)$$

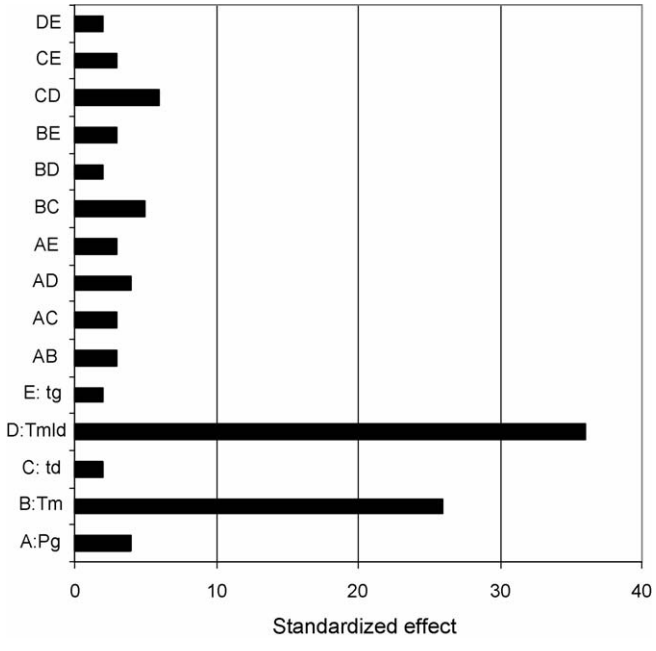

Fig. 8. Pareto chart showing the effect of each controlled variable.

From previous investigations [5,8] it is known that the gas penetration length increases in parallel to the delay time. An increase in the delay time means more time for the polymer to cool down, and thus a greater polymer frozen layer is generated. As a result, the gas drags a smaller transversal area of polymer but during a longer penetration length. In our case, the delay time seems to have minor importance on the amount of the solidified polymer layer. In fact, we cannot appreciate significant differences when low or high delay times were selected. This is probably caused by the slim range of tested delay times, although higher values for the delay time would render short-shots.

No variable influence was observed when dealing with part thickness at the beginning, middle or ending points of the gas channel. This fact implies that the wall plastic thickness next to the gas channel is difficult to be modified through changes in the processing parameters, so a carefully geometric design needs to be performed prior to mould manufacturing.

From the simulation it can be concluded that the part weight is minimised when the melt and mould temperatures are situated at their higher values. This is reasonable because both factors decrease the polymer viscosity and the gas could take out a greater quantity of polypropylene. As expected, the gas

pressure plays the most important role followed by the melt and the mould temperatures. These three variables control the gas-injection process of the studied cover.

5.4. Contrast between simulation and real part manufacturing

The results obtained from the gas-assisted injection simulation where compared with the cover once it was industrially produced. Some differences were introduced in the manufacturing process according to the features observed in the simulation. The principal difficulty to overcome was the predicted intrusion of gas near the melt entrance (Fig. 7a). To solve this problem the gas entrances where finally displaced towards the part corners, up to a position near to that shown in Fig. 6c. Furthermore, in order to avoid gas bridging between the two inlet points, only one gas inlet point on each side of the part was used. The voiding was assured because during the simulations the best hollowing part control was obtained with two channels and this configuration was the one finally used. The comparison between fabrication and simulation has to be taken in a qualitative manner because the final gas-injection layout alternative and the final geometry were slightly modified according to the previous results.

In the fabricated cover (Fig. 9) there were no signs of skin roughness or welding lines and no distortion or warp due to unbalanced shrinkage was observed. The differences between melt velocities in and out of the channel were not significant in terms of skin marks due to back flow. Regarding melt voiding the channels were completely empty of polymer along their entire length. As expected, it was not possible to foresee the thickness along the gas path by a change in the processing parameters. In the results shown in Table 6 it can be appreciated that similar channel thicknesses were achieved applying different input parameters.

If the thickness at the initial point of the gas channel are considered (T_1 in Table 6), it can be appreciated that the predicted

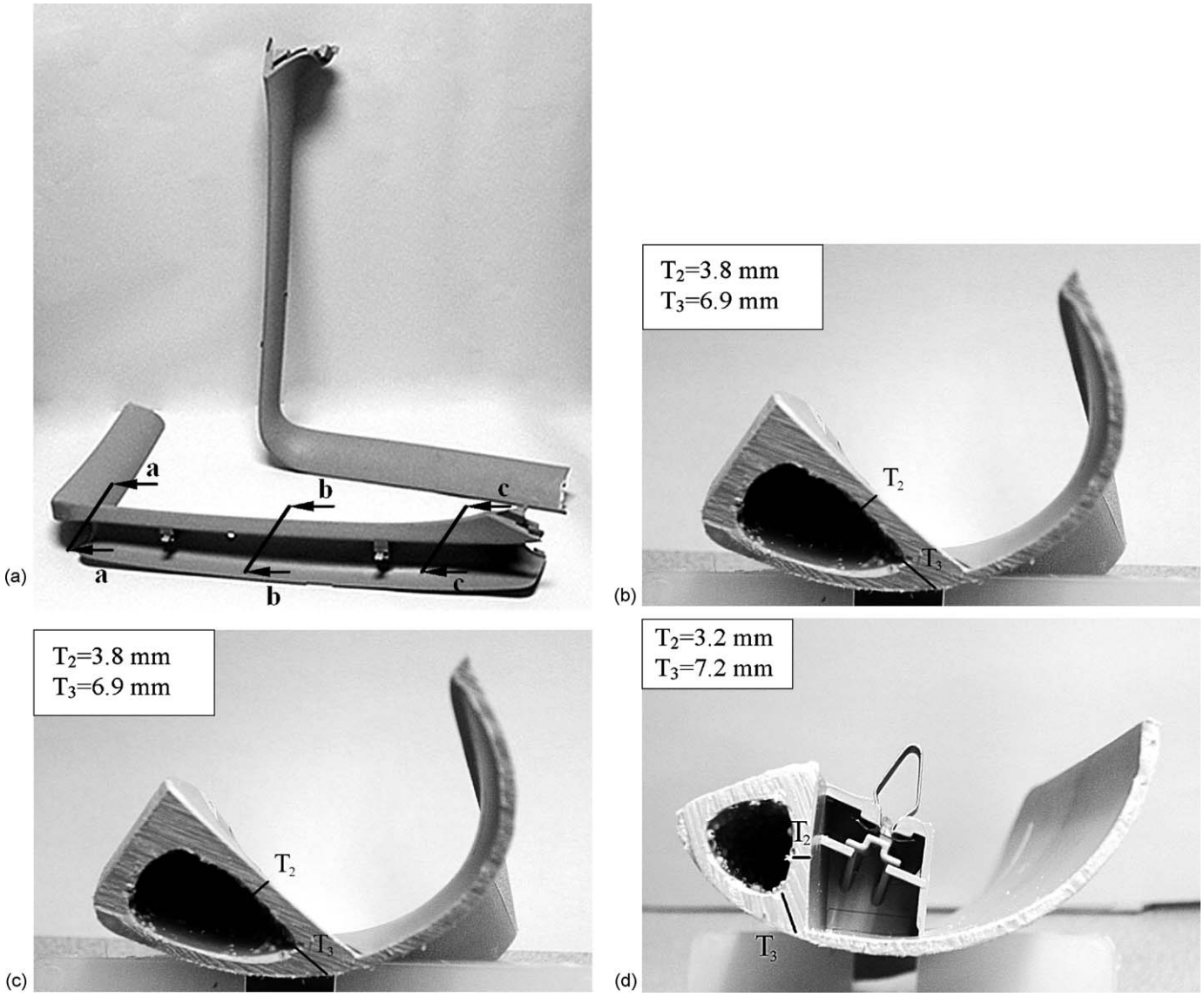

Fig. 9. (a) Photograph of the two mid-sides of the transformed cover showing the positions of different tails taken for thickness observation. Detail of the gas channel thickness at the indicated sections. (b) Section a–a. (c) Section b–b. (d) Section c–c.

polymer skin is very low and therefore gas could break the polymer layer leaving a hole in the part. However, it is necessary to remark that the control point was situated just by the gas inlet and so the polymer skin layer was very slim. At the testing point in the injected part, the thickness varies from a maximum of about 0.96 mm to a minimum of 0.70 mm. The thickness of the channel wall at the internal side of the part (T_2), measured at different positions of the channel length (Fig. 9) results in values of around 3.5 mm, which were coincident with the predicted ones that are collected in Table 6. Again, changes in the input parameters do not render significant changes in the channel thickness at an intermediate position except for those situations where channel voiding was not achieved. Differences of about 0.4 mm were found to be between the polypropylene transversal sections at position T_3 versus the simulated ones. The minimum polymer layer thickness in this zone was about 6.9 mm (Fig. 9) whereas the simulation yield values were between 6.52 and 7.08 mm, this being considered equal to the real thickness. The closeness of the predicted thickness values do not allow for the selection of the best combination for the input parameters, but permits discarding the combinations with excessive polymer layer which coincide with the options with minimum channel voiding.

6. Conclusions

The gas simulation is a powerful tool to optimise the production of thick plastic parts. Several alternatives were contrasted in order to find the best solution to fabricate a plastic automobile cover. The best part arrangement was achieved when a central point injected the plastic melt and two lateral points close to the former applied gas. The injection simulation with a sole central point resulted in a good temperature distribution but a long melt path and great pressure losses avoiding the presence of weld lines and the risk of early failure. The selected position for the gas-injection assured the melt was totally removed from the gas-channel and implied a simple mould execution. In terms of part hollowing, greater polymer volumes were removed from the part as the gas pressure and melt and mould temperatures were increased. The features observed during the gas simulation were used to modify the final part design. A very good match was observed between simulation trends and the real gas-injection process although no quantitative direct comparison was realised.

Acknowledgement

The authors wish to thank Centre de Referència en Tècniques Avançades de Producció (CeRTAP) of the Generalitat de Catalunya (Catalonian Government) for the financial support of this work.

References

[1] J. Avery, Injection Molding Alternatives, Hanser Publishers, Munich, 1998.
[2] G. Pötch, W. Michaeli, Injection Molding: An Introduction, Hanser Publishers, Munich, 1995.
[3] J. Ehritt, K. Schröeder, Gas Injection and Two-component Injection Moulding, Hüthig-Battenfeld, Heidelberg, 1995.
[4] J. Avery, Gas-assist Injection Molding: Principles and Applications, Hanser Publishers, Munich, 2001.
[5] C.T. Li, J.W. Shin, A. Isayev, H.S. Lee, Primary and secondary gas penetration during gas-assisted injection molding. Part II. Simulation and experiment, Polym. Eng. Sci. 44 (2004) 992–1002.
[6] S.J. Liu, K.H. Chang, Parameters affecting the full-shot molding of gas-assisted injection-molded parts, Adv. Polym. Technol. 22 (2003) 1–14.
[7] S.Y. Yang, C.T. Lin, J.H. Chang, Secondary gas penetrations in ribs during full-shot gas-assisted injection molding, Adv. Polym. Technol. 22 (2003) 225–237.
[8] M.A. Parvez, N.S. Ong, Y.C. Lam, S.B. Tor, Gas-assisted injection molding: the effects of process variables and gas channel geometry, J. Mater. Process. Technol. 121 (2002) 27–35.
[9] C-MOLD, Advanced CAE Technology, Inc., Ithaca, NY, USA, 1995.
[10] G.E.P. Box, W.G. Hunter, J.S. Hunter, Statistics for Experimenters: An Introduction to Design, Data Analysis, and Model Building, John Wiley & Sons, New York, 1978.
[11] J. Lahey, R. Launsby, Experimental Design for Injection Moulding, Launsby Consulting, Colorado, 1998.
[12] International Standards Organisation, ISO 3795, Road vehicles, and tractors and machinery for agriculture and forestry, Determination of burning behaviour of interior materials, 1989.
[13] M.L. Williams, R.F. Landel, J.D. Ferry, The temperature dependence of relaxation mechanism in amorphous polymers and other glass-forming liquids, J. Am. Chem. Soc. 77 (1955) 3701–3707.
[14] H.H. Chiang, C.A. Hieber, K.K. Wang, A unified simulation of the filling and postfilling stages in injection molding. Part I. Formulation, Polym. Eng. Sci. 31 (1991) 116–124.
[15] B. Hartmann, R. Simha, A.E. Berger, PVT scaling parameters for polymer melts, J. Appl. Polym. Sci. 37 (1989) 2603–2616.
[16] B. Hartmann, R. Simha, A.E. Berger, PVT scaling parameters for polymer melts. II. Error in all variables, J. Appl. Polym. Sci. 43 (1991) 983–991.
[17] R.K. Jain, R. Simha, Theoretical equation of state: thermal expansivity, compressibility, and the Tait relation, Macromolecules 22 (1989) 464–468.
[18] E.B. Bagley, End corrections in the capillary flow of polyethylene, J. Appl. Phys. 28 (1957) 624–627.
[19] A. Gordillo, M.Ll. Maspoch, M. Sánchez-Soto, G. Bugeda, X. Royo, R. Aubry, M. Chiumenti, V. Vivancos, R. Morales, Experimental verification of 3d injection molding simulation, in: Proceedings of the Sixth International Research/Expert Conference, Trends in the Development of Machinery and Associated Technology (TMT 2002), Neum, 2002.